Ieva Švagždytė ✉
Sergejus Borodinas
Artūras Kilikevičius
Vadim Mokšin

https://doi.org/10.21278/TOF.452010119
ISSN 1333-1124
eISSN 1849-1391

INVESTIGATION INTO LEVITATING POLISHING DISC USED FOR FLAT SURFACE FINISHING

Summary

The paper presents a new type of flat surface polishing device. The polishing disc rotates using the pressure of compressed air. The polishing disc has a special geometry, wherein it has holes for flow turbulence minimisation in the air pressure areas of the boundary. The influence of the hole inclination angle on the rotational speed of the disk and the system efficiency was studied experimentally and numerically. It was established that the optimal inclination angle is a 20° angle that results in the maximum efficiency of the proposed system. In the experiment, three polishing discs with hole inclination angles of 0°, 20°, and 30° were studied; the discs were rotated using four air pressure values: 0.2, 0.3, 0.4, and 0.5 MPa. It was found that the optimal inclination angle of holes was 20° and that the fastest rotational speed, i.e. 1900 1/min, was reached at a maximum air pressure of 0.5 MPa.

Key words: *polishing efficiency, flat surface polishing device, polishing disc rotational speed, compressed air*

1. Introduction

Polishing is usually the final machining operation used for parts with high surface quality. This process is especially important for optical elements, such as lenses, mirrors, and prisms. The spread of light through optical elements depends on the internal structure and surface quality of the crystal (or optical glass). There are a few parameters that describe surface quality, and two of the most important ones are surface roughness and shape deviation.

There are only a few types of machine tools for polishing flat optical components. The most often used polishing process is chemical mechanical polishing, where a rotating workpiece is polished on a conventional eccentric single-arm spindle polisher with a polyurethane pad [1, 2]. Parameters, such as polishing head speed, pressure, overarm speed [3], and polishing time need to be determined. Depending on these parameters, it is possible to vary the material removal rate (MRR) and surface quality. As the entire workpiece area is in contact during the polishing process, the geometry of the polishing pad influences the polished surface. A novel dual-axis disc polishing system using semi-rigid polishing

presented in [4] allows the polishing efficiency to be increased and the process cycle time to be reduced. The contact area depends on the polishing disc width and only this area is involved in the processing during polishing. A combination of this method and magnetorheological finishing (MRF) and hydrodynamic effect polishing (HEP) is presented in [5] for ultra-precision optical manufacturing. The first experimental results showed that the surface spatial frequency error and surface roughness were reduced. Due to these reasons, a new method was proposed and applied.

Process parameters such as the polishing head speed, pressure, overarm speed, slurry flow rate, polishing time, slurry temperature, abrasive concentration, abrasive size, and the parameters obtained after the polishing process (such as the MRR and surface roughness), were fully described. To optimise the polishing process, scientists test various parameter combinations using Taguchi's L9 orthogonal array for the design of experiments [1, 3] and apply the in-process monitoring of the surface shape [6]. The process parameters were determined for a high-quality quartz glass substrate undergoing chemical mechanical polishing. The MRR was 56.8 nm/min and the surface roughness (*Ra*) was 0.193 nm when the pressure was 5171 Pa, the polishing head speed was 65 1/min, the platen speed was 60 1/min, the slurry flow rate was 150 mL/min, the slurry temperature was 20 ^{o}C, and the polishing time was 60 s [7]. In their study, Belkhir et al. showed that during the polishing process, it is essential to control the contact pressure and the polisher shape according to pressure distribution to guarantee a very high quality of the polished surface [8]. In the experimental study into the full aperture polishing of BK7 optical glass with cerium oxide slurry, it was established that the pressure applied to the workpiece–polisher interface affected the MRR, but the pressure variation did not have any significant effect on the surface roughness [3]. Other experimental results showed that ultra-smooth uniform polishing can significantly improve the mid- and the high-spatial frequencies of roughness without destroying the surface figure of high-precision optical components [9]. In the study, a compressive set of 100 mm diameter glass workpieces (fused silica, phosphate, and borosilicate) were polished, and the results indicated that the dominant factor influencing surface roughness is the slurry particle size distribution, followed by the removal function of the glass material and pad topography [10]. Monocrystalline 6H-SiC and Si wafers were polished by combining MRF with a cluster mechanism. Abrasives of different grain sizes had the same effect on the processed surface [11]. Plasma-assisted polishing, which combines plasma modification with soft abrasive polishing and can be used for gallium nitride polishing was investigated in [12], and a wet pad surface was characterised with ultra-high resolution full-field optical coherence tomography (FF-OCT) in [13].

To avoid faults in the polishing process, scientists develop systems that allow more precise control of the process itself and its quality. A serial parallel hybrid polishing machine tool is introduced in [14]; it consists of a parallel mechanism of a three-dimensional moving platform, a serial rotational mechanism of two degrees of freedom and an elastic polishing tool system. Systems that automatically control the polishing time and the loading force of the polishing tool are used in [15]. Scientists pay a lot of attention to the processing of complex shapes. An integrated polishing process system for finishing primary and tertiary mirrors is introduced in [16], and a self-optimization system for corrective polishing of optical freeform surfaces in [17]. These and similar systems require large investments and highly skilled workers.

In all of these polishing techniques, kinematic relations and geometry are important for the polished surface quality. The accuracy of the polishing machine and the polishing pad geometry directly influence the polished surface quality of. In this paper, a new type of polishing device is proposed for a highly efficient polishing process of a flat optical surface.

2. Research Subject

The designed flat surface polishing device can be used for polishing flat surfaces, which have to satisfy high accuracy and smoothness requirements. The aim of this study is to improve the quality of polishing and to enhance productivity. The flat surface polishing device is protected by Patent LT 6564 B of the Republic of Lithuania [18]; the patented polishing disc which rotates using compressed air does not have kinematic joints with other parts of the device. It consists of a Venturi tube (2) placed in a hollow housing (1) (Fig. 1). The confusor (3) of the Venturi tube is connected to the lower wall (4) of the housing. The polisher holder (10) and the polisher (11), which is attached eccentrically, are placed in the ring (9) attached to the wide lower side of the housing (8). The polisher holder (10) and the polisher (11) have holes (12) and (13) that are joined. Slurry is fed through the hole (15) in the wide side of the lower part of the housing (8) and the holes (14) drilled in the polisher holder (10). The tangential holes (17) in the inner side of the wall (16) are formed near the middle of the vertical wall (18) of the polisher holder (10). There are vertical edges on the surface of the wall (18) that are parallel to the rotary axis (19); their height and number depend on the required torque of the polisher. Diameter $D1$ of the inside wall (16) of the ring is greater than external diameter $D2$ of the wall (18) of the polisher holder (10) by value Δ. The movement of the polisher holder (10) along the axis is limited by the cover (20) that is mounted on the ring (9); the inside diameter of the cover should not be greater than $D1 - 2\Delta$.

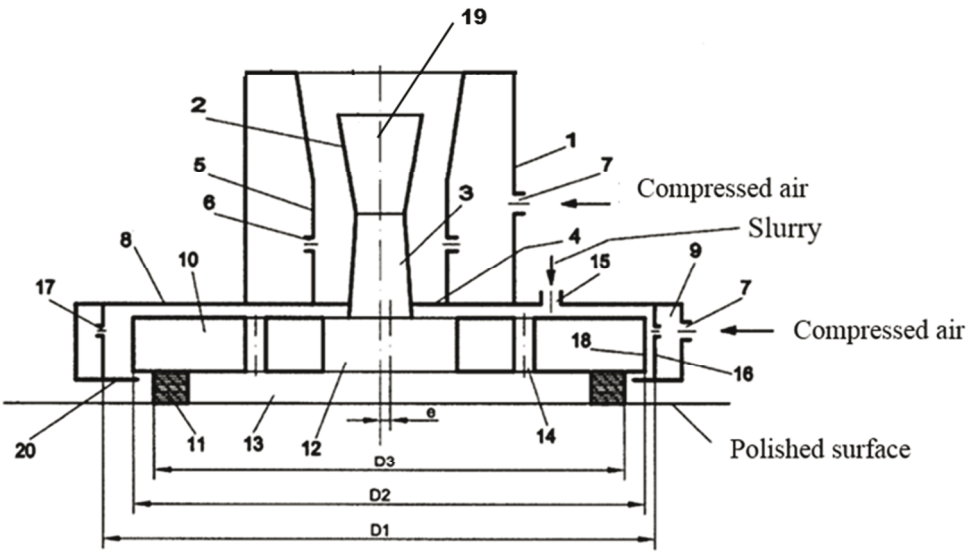

Fig. 1 Schematic diagram of the flat surface polishing device

The device should be placed on the workpiece being polished and the polisher (11) should touch the surface of the workpiece. Slurry is fed through the hole (15). Compressed air is supplied through the hole (7). Then, the compressed air passes the tangential holes (17) and the flow eddies are formed near the surface (18) of the holder. The flows give a complex trajectory to the polisher holder (10) with the polisher (11): rotation about the axis of the housing (19), an extra rotation about the polisher axis (11) shifted by eccentricity e from the housing axis (19), and radial oscillations of the polisher holder (10). The oscillations of its axis with amplitude Δ increase the quality of the polished surface and avoid the repetition of the trajectory of the polisher (11) on the workpiece surface. Extra oscillations allow improvement in the process efficiency without increasing the pressure of the polisher (11) and grain size of the slurry. In the hole (13), a stable film of polishing slurry is formed due to the

interaction between two opposite air flows formed by the tangential holes (6) and (17). It is possible to enhance the polishing process efficiency by changing the ratio between air flows without decreasing the polishing process quality.

3. Numerical Simulation

Rotational movements of the polisher holder are studied and discussed in this paper. As the system utilizes compressed air, the turbulence of the air flow influences the friction coefficient [19] and the quality of the whole system. The compressed air inlet is designed at an angle to the rotation axis, i.e. it is inclined, similar to the nozzles of the stator inlets of Tesla turbines [20, 21]. The polisher holder is designed as a polishing disc with a specific geometry that includes holes for the air outlet.

The current model represents a polishing disc with eight outer boundaries for activating rotational movements, which depend on the air pressure, as shown in Fig. 2. The rotating disc inside the housing has clearance between the walls and can be represented as a pump. The assembled 3-dimensional model shown in Fig. 2 includes a tangential inlet for external air pressure connection and an outlet at the bottom of the cover. The rotating polishing disc is designed for one-way (clockwise) rotation. Each external boundary shape has a hole for turbulent flow minimisation in the air pressure area of the boundary, as shown in Fig. 2.

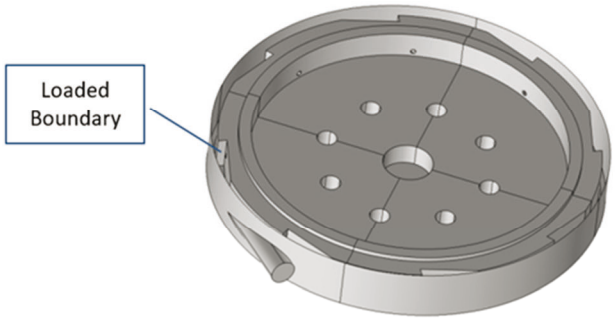

Fig. 2 Geometry of semi-open rotating polishing disc assembly

The main goal of the numerical simulation is to find an optimal angle between the *x* axis of the disc and the axis of the hole, as shown in Fig. 3. Among the available computational tools, the COMSOL Multiphysics software applies the finite element method to solve physics and engineering problems (e.g. rotating machinery) governed by partial differential equations. The rotating machinery and transient multiphysics combine the turbulent flow and the *k-ω* interface and are used to simulate a flow at high Reynolds numbers in geometries with one or more rotating parts. The physics interface is suitable for incompressible and compressible flows at low Mach numbers (in our study, the Mach number is less than 0.2).

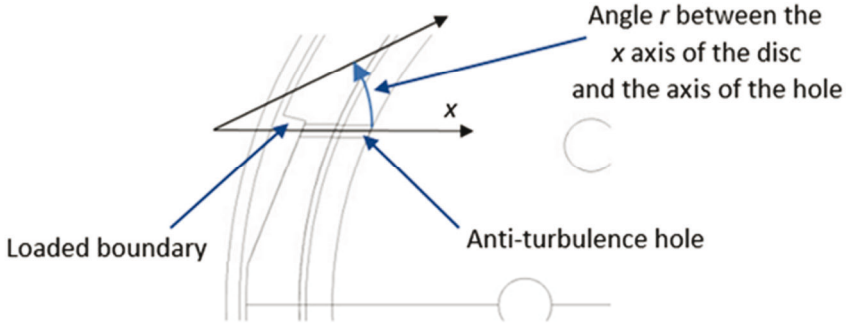

Fig. 3 Graphic representation of the anti-turbulence hole angle *r* (the shown angle is 0^{o})

The geometry used in this study is highly parameterised to allow for easy modification of the geometry (hole angles) required to study different configurations of the polishing disc. A dedicated multiphysics coupling condition is readily defined for the air-solid boundary; this condition sets up the air loads on the solid domain and the effect of structural accelerations on the air. Each module is governed by its own equations that describe the specific physics.

The turbulence effects are modelled using the Wilcox revised two-equation k-ω model with realisability constraints. This is a widely-used model for turbomachinery simulations, with good performance for swirling flows in the near-wall region. The momentum balance is governed by the Navier–Stokes equations, and the mass conservation is governed by the continuity equation. This model uses rotating machinery simulation with the frozen rotor approach for the rotating polishing disc. The frozen rotor is a cost-effective and time-efficient steady-state approximation, where different rotational speeds are assigned to individual zones. The flow in each of these zones is solved using the moving reference frame equations. Using the frozen-rotor study type, the rotating parts are kept frozen in position, and the rotation is accounted for by the inclusion of centrifugal and Coriolis forces.

The mass flow ($\dot{m}$) is monitored using two probe plots, one at the inlet and the other at the outlet. Mass conservation is achieved when the mass flows at the inlet and outlet are equal. Choosing the right angular position of the hole maximises the system efficiency. The rotating polishing disc efficiency is calculated by dividing the fluid power with the shaft power consumption. An additional probe plot is used for calculating the air pressure load on the working boundary during rotation. By maximising this value, higher system efficiency can be achieved.

In the current physics interface, we used a moving mesh and a rotating domain setup. For the first step in the numerical calculation, the rotating speed was set to 3000 1/min with a constant pressure of 200 000 Pa at the inlet, and a varying hole angle (from 0 to 30^{o} with a 5^{o} step). The velocity magnitude with one angle position is shown in Fig. 4, which represents the air swirling flow distributions in the system.

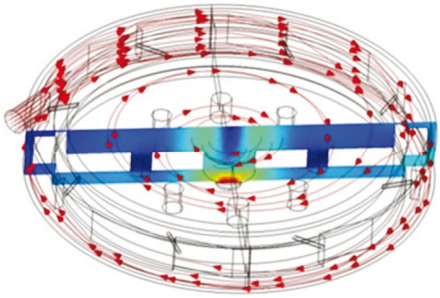

Fig. 4 Velocity magnitude representing the air swirling flow distributions in the system

The normalised graphs of the system efficiency and accumulated boundary loads are shown in Fig. 5. We can assume that the maximum values are achieved when the hole angle is 20°.

Based on the numerical calculation, the Reynolds number of our system is higher than 7000. In fluid dynamics, the critical velocity is also represented in terms of the critical Reynolds number. This means that the kinetic energy per unit mass is associated with eddies in a turbulent flow, and the turbulence kinetic energy (TKE) is characterised by velocity fluctuations. By incorporating this additional velocity component in the Navier–Stokes equations and rearranging, additional terms can be found; they resemble viscous stresses, and these are referred to as the Reynolds stresses. Based on this assumption, a correlation can be established between the anti-turbulence hole angle and TKE to find the optimal angle of the holes.

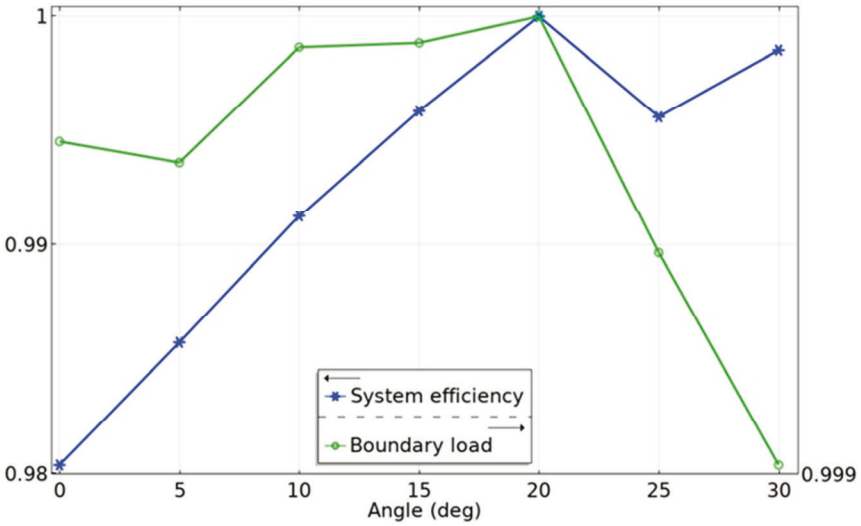

Fig. 5 Normalised system efficiency (blue) and boundary load (green, see Fig. 2) as functions of the hole inclination angles

The normalised TKE at the outlet is shown in Fig. 6. We can see that the minimum value is achieved when the hole angle is 20° at a constant rotor speed of 3000 1/min. These eddies then decay into smaller eddies that carry less kinetic energy (depending on the hole angle), until the viscous forces eventually reach a minimum (20°–purple line).

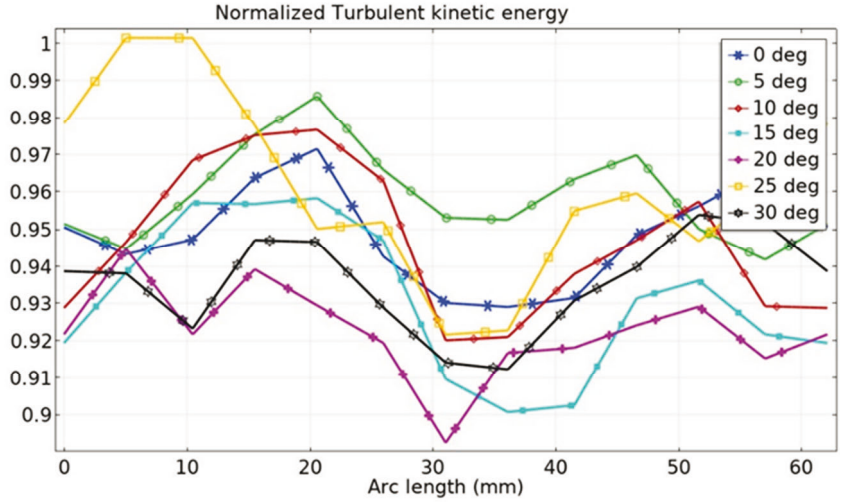

Fig. 6 Normalized TKE obtained for different hole inclination angles

Based on the results of our previous numerical simulation, we can assume that anti-turbulence holes made at the boundary loaded by air pressure influence the system efficiency. We found that their optimal inclination angle is approximately 20°, which corresponds to the maximum efficiency of the proposed polishing system. The efficiency of the optimised system (the inclination angle is 20°) depends on the rotational speed and the inlet pressure as shown in Fig. 7. This figure depicts high linearity in a wide range of parameter changes.

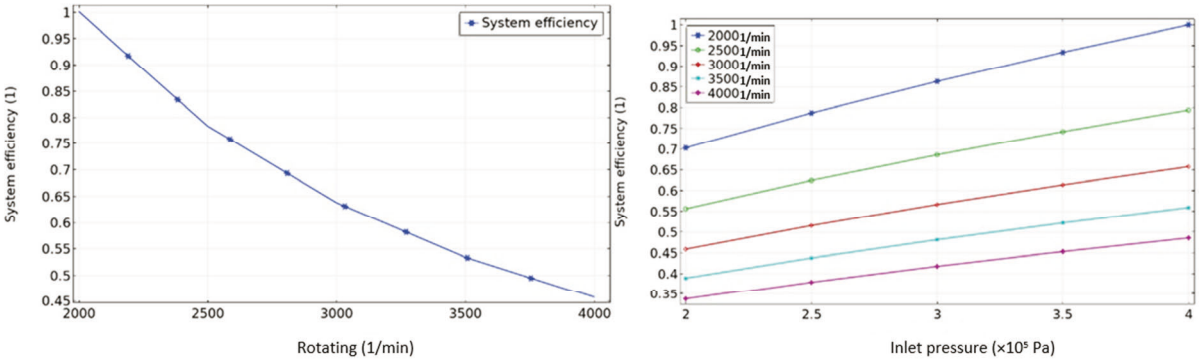

Fig. 7 Efficiency of the optimised system as a function of the rotating speed (left) and the inlet pressure (right)

4. Experiment

The dependence of rotational speed on the polishing disc geometry and air pressure was studied experimentally. Three polishing discs were manufactured (Fig. 8) with different hole inclination angles of 0°, 20°, and 30°. The polishing discs made of organic glass had 152 mm in diameter.

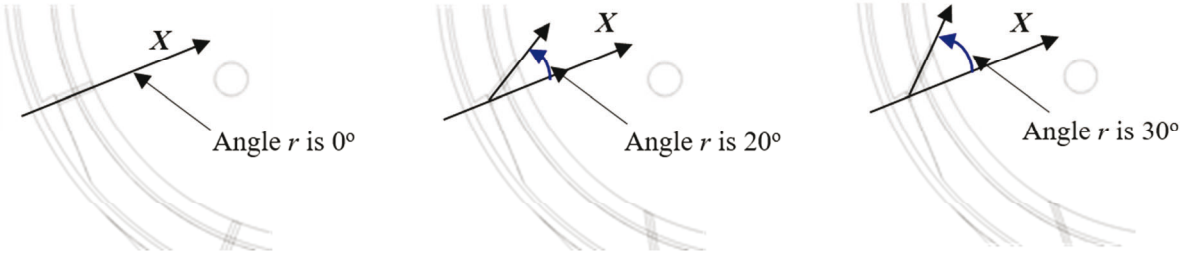

Fig. 8 Polishing discs with different hole angles (from left to right): 0^0, 20^0 and 30^0

A scheme of the experimental stand for measuring the polishing disc rotational speed is shown in Fig. 9(a). A manometer and an MM-0024 photo-electronic tachometer probe were used for measurements. A photo of the stand with a Bruel&Kjaer machine diagnostics toolbox, type 9727, is shown in Fig. 9(b).

The flat surface polishing device (4) is placed on the surface to be polished (1). Compressed air passes through the inlet (2) into the stand. Air pressure is regulated using the valve (7) and measured by the manometer (3). In experiments, the compressed air pressure was varied from 0.2 to 0.5 MPa. These values are generally used in factories and companies for processing different types of surfaces, such as glass, metal, plastics, and ceramics. The MM-0024 photo-electronic tachometer probe (5) provides a pulse of infrared light to the rotating polishing disc and receives the reflection of light. Finally, the results of the measurements are sent to the computer, which is connected to the machine diagnostics toolbox, type 9727 (6).

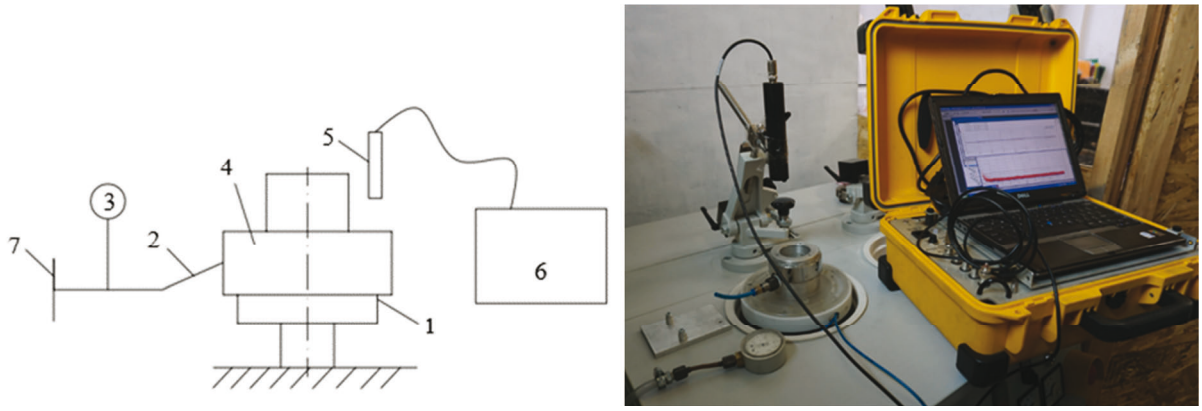

a) b)

Fig. 9 Experimental stand used to measure the rotational speed of polishing disc (a – scheme of the experimental stand, b – photo of the stand); 1 – polished surface; 2 – compressed air inlet; 3 – manometer; 4 – prototype of flat surface polishing device; 5 – MM-0024 photo-electronic tachometer probe; 6 – Machine diagnostics toolbox, type 9727, with a DELL computer; 7 – air pressure regulation valve

Results of experiments are presented in Fig. 10. One can see that the rotational speed of polishing disc increases with an increase in the supplied air pressure.

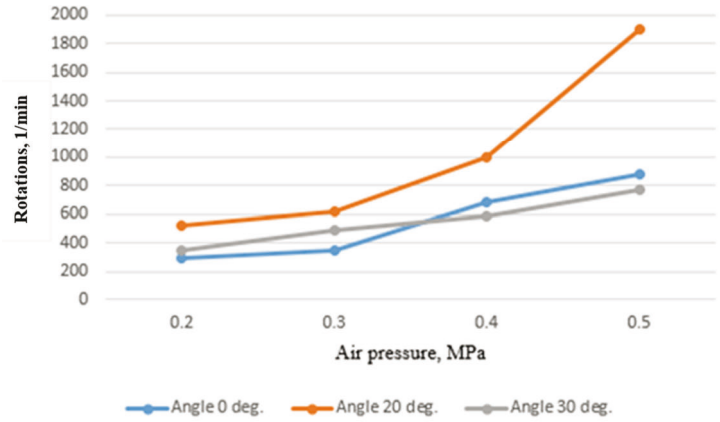

Fig. 10 Rotational speed of polishing disc versus hole inclination angle and air pressure

It is clear from Fig. 10 that the rotational speed of the polishing disc increases gradually, and that the highest rotational speeds are obtained at the maximum air pressure, i.e. at 0.5 MPa. Polishing discs with hole inclination angles of 0° and 30° rotated at similar speeds of 885 and 768 1/min, respectively, when the air pressure was 0.5 MPa. Rotational speeds of the polishing disc with a hole inclination angle of 20° were higher than those obtained for the other two discs; the slowest rotational speed was 527 1/min when the air pressure was 0.2 MPa, and the fastest rotational speed was 1900 1/min when the air pressure was 0.5 MPa. The results of the experiments confirm the numerical simulation results which show that the optimal angle of holes to achieve the highest efficiency of the rotating part in the proposed flat surface polishing device is the 20° angle.

5. Conclusions

A new type of flat surface polishing device with improved efficiency and quality of the polishing process is proposed. The polishing disc rotates using compressed air without any kinematic relations with other parts of the polishing device.

Polishing discs with different hole inclination angles for the air outlet were investigated to reduce the turbulence.

Based on the numerical simulation results, it was established that anti-turbulence holes made in the boundary loaded by air pressure influence the system efficiency. It was found that their optimal inclination angle is approximately 20°, which corresponds to the maximum efficiency of the proposed system of the rotating polishing disc.

The experimental results confirm the numerical simulation results showing that the optimal inclination angle of holes is a 20° angle. The polishing disc with hole inclination angles of 20° reached higher rotational speeds than the other two discs with hole inclination angles of 0° and 30°. The lowest rotational speed obtained for a minimum air pressure of 0.2 MPa was 527 1/min and the highest rotational speed obtained for a maximum air pressure of 0.5 MPa was 1900 1/min. Finally, it was possible to achieve the highest efficiency of the rotating disc in the proposed flat surface polishing device.

REFERENCES

[1] Singh, A., Garg, H., Kumar, P., Lall, A.K. Analysis and optimization of parameters in optical polishing of large diameter BK7 flat components, *Materials and Manufacturing Processes* **2017**, 32 (5), 542-548. https://doi.org/10.1080/10426914.2016.1221103

[2] Singh, A., Garg, H., Lall, A.K. Optical polishing process: Analysis and optimization using response surface methodology (RMS) for large diameter fused silica flat substrates, *Journal of Manufacturing Processes* **2017**, 30, 439-451. https://doi.org/10.1016/j.jmapro.2017.10.017

[3] Pal, R.K., Garg, H., Sarepaka, R.V., Karar, V. Experimental investigation of material removal and surface roughness during optical glass polishing, *Materials and Manufacturing Processes* **2016**, 31 (12), 1613-1620. https://doi.org/10.1080/10426914.2015.1103867

[4] Lu, A., Jin, T., Guo, Z., Qu, M., Chang, Y., Liu, Q., Zhang, C. Characterization of the tool influence function in a dual-axis wheel polishing process to achieve high material removal rates, *Precision Engineering* **2018**, 52, 276-290. https://doi.org/10.1016/j.precisioneng.2018.01.003

[5] Peng, W., Li, S., Guan, C., Li, Y., Hu, X. Ultra-precision optical surface fabricated by hydrodynamic effect polishing combined with magnetorheological finishing, *Optik* **2018**, 156, 374-383. https://doi.org/10.1016/j.ijleo.2017.11.055

[6] Filatov, Yu.D., Sidorko, V. I., Kovalev, S.V., Filativ, O.Yu., Monteil, G. In-Process monitoring of shape accuracy of flat surfaces of optical and microelectronic components in polishing, *Journal of Superhard Materials* **2017**, 39 (4), 282-287. https://doi.org/10.3103/s1063457617040086

[7] Bo, D., Jianwei, Z., Yuling, L., Mingbin, S., Yufeng, Z. Surface roughness of optical quartz substrate by chemical mechanical polishing, *Journal of Semiconductors* **2014**, 35, 116001. https://doi.org/10.1088/1674-4926/35/11/116001

[8] Belkhir, N., Aliouane, T., Bouzid, D. Correlation between contact surface and friction during the optical glass polishing, *Applied Surface Science* **2014**, 288, 208-214. https://doi.org/10.1016/j.apsusc.2013.10.008

[9] Ma, Z., Peng, L., Wang, J. Ultra-smooth polishing of high-precision optical surface, *Optik* **2013**, 124, 6586-6589. https://doi.org/10.1016/j.ijleo.2013.05.093

[10] Suratwala, T., Steele, W., Feit, M., Shen, N., Dylla-Spears, R., Wong, L., Miller, P., Desjardin, R., Elhadj, S. Mechanism and simulation of removal rate and surface roughness during optical polishing of glasses, *Journal of the American Ceramic Society* **2016**, 99 (6), 1974-1984. https://doi.org/10.1111/jace.14220

[11] Pan, J., Yan, Q. Material removal mechanism of cluster magnetorheological effect in plane polishing, *The International Journal of Advanced Manufacturing Technology* **2015**, 81, 2017-2026. https://doi.org/10.1007/s00170-015-7332-7

[12] Deng, H., Endo, K., Yamamura, K. Plasma-assisted polishing of gallium nitride to obtain a pit-free and atomically flat surface, *CIRP Annals – Manufacturing Technology* **2015**, 64, 531-534. https://doi.org/10.1016/j.cirp.2015.04.002

[13] Choi, W.J., Jung, S.P., Shin, J.G., Yang, D., Lee, B.H. Characterization of wet pad surface in chemical mechanical polishing (CMP) process with full-field optical coherence tomography (FF-OCT), *Optics Express* **2011**, 19 (14), 13343-13350. https://doi.org/10.1364/oe.19.013343

[14] Wang, G., Wang, Y., Zhao, J., Chen, G. Process optimization of the serial-parallel hybrid polishing machine tool based on artificial neutral network and genetic algorithm, *Journal of Intelligent Manufacturing* **2012,** 23, 365-374. https://doi.org/10.1007/s10845-009-0376-5

[15] Liu, W., Chi, Y., Li, M., Tong, H. Research on control system of new type ceramic polishing machine, *Second International Conference on Mechanic Automation and Control Engineering* **2011.** https://doi.org/10.1109/mace.2011.5987240

[16] Zhang, L., Huang, D., Zhou, W., Fan, C., Ji, S., Zhao, J. Corrective polishing of freeform optical surfaces in an off-axis three-mirror imaging system, *The International Journal of Advanced Manufacturing Technology* **2017,** 88, 2861-2869. https://doi.org/10.1007/s00170-016-8995-4

[17] Cao, Z.C., Cheung, C.F., Liu, M.Y. Model-based self-optimization method for form correction in the computer controlled bonnet polishing of optical freeform surfaces, *Optics Express* **2018,** 26 (2), 2065-2078. https://doi.org/10.1364/oe.26.002065

[18] Svagzdyte, I., Striska, V., Jurevicius, M., Krickas, L., Kilikevicius, A. Flat surface polishing device. Patent LT 6564 B of Republic of Lithuania, **2018**.

[19] Ohta, T. Turbulence structures in high-speed air flow along a thin cylinder, *Journal of Turbulence* **2017**, 18 (6), 497-511. https://doi.org/10.1080/14685248.2017.1298769

[20] Talluri, L., Fiaschi, D., Neri, G., Ciappi, L. Design and optimization of a Tesla turbine for ORC applications, *Applied Energy* **2018**, 226, 300-319. https://doi.org/10.1016/j.apenergy.2018.05.057

[21] Song, J., Gu, C., Li, X. Performance estimation of Tesla turbine applied in small scale Organic Rankine Cycle (ORC) system, *Applied Thermal Engineering* **2017**, 110, 318-326. https://doi.org/10.1016/j.applthermaleng.2016.08.168

Submitted: 30.10.2019

Accepted: 22.4.2021

lect. Ieva Švagždytė
Department of Mechanical and Materials Engineering
Vilnius Gediminas Technical University
Basanavičiaus str. 28, Vilnius, Lithuania

assoc. prof. Sergejus Borodinas
Department of Applied Mechanics
Vilnius Gediminas Technical University
Saulėtekio ave. 11, Vilnius, Lithuania

assoc. prof. Artūras Kilikevičius
Institute of Mechanical Science
Vilnius Gediminas Technical University
Basanavičiaus str. 28, Vilnius, Lithuania

prof. Vadim Mokšin
Department of Mechanical and Materials Engineering
Vilnius Gediminas Technical University
Basanavičiaus str. 28, Vilnius, Lithuania